DE GRUYTER OPEN

***MINERALOGIA**, 46, No 1-2: 41-50 (2015)*
DOI: 10.1515/mipo-2017-0001
www.Mineralogia.pl

MINERALOGICAL SOCIETY OF POLAND
POLSKIE TOWARZYSTWO MINERALOGICZNE

Original paper

Ba- and Ti-enriched dark mica from the UHP metasediments of the Seve Nappe Complex, Swedish Caledonides

Jarosław Majka[1,2*], Łukasz Kruszewski[3], Åke Rosén[4], Iwona Klonowska[1]

[1] *Uppsala University, CEMPEG – Department of Earth Sciences, Villavägen 16, SE – 752 36 Uppsala, Sweden*
[2] *AGH – University of Science and Technology, Faculty of Geology, Geophysics and Environmental Protection, al. Mickiewicza 30, 30-059 Kraków, Poland*
[3] *Polish Academy of Sciences, Institute of Geological Sciences, ul. Twarda 51/55, 00-818 Warszawa, Poland*
[4] *University of Bern, Institute of Geological Sciences, Baltzerstrasse 1+3, CH-3012 Bern, Switzerland*
** Corresponding author: jaroslaw.majka@geo.uu.se*

Received: January 25, 2016
Received in revised form: September 15, 2016
Accepted: October 10, 2016
Available online: February 10, 2017

Abstract. We report on the occurrence of peculiar Ba- and Ti-enriched dark mica in metasedimentary rocks that underwent high-pressure metamorphism in the diamond stability field followed by decompression to granulite facies conditions. The mica occurs as well-developed preserved laths in a quartzofeldspathic matrix. The mean concentrations of BaO and TiO_2 in the mica are 11.54 and 7.80wt%, respectively. The maximum amounts of these components are 13.38wt% BaO and 8.45wt% TiO_2. The mean crystallochemical formula can be expressed as $(K_{0.54}Ba_{0.39}Na_{0.02}Ca_{0.01})_{\Sigma 0.96}(Fe_{1.37}Mg_{0.85}Ti_{0.50}Al_{0.29}Mn_{0.01}Cr_{0.01})_{\Sigma 3.03}(Si_{2.59}Al_{1.41})_{\Sigma 4.00}O_{10}(OH_{1.30}O_{0.66}F_{0.02}S_{0.01})_{\Sigma 1.99}$, with *oxyannite*, *oxy-ferrokinoshitalite* and siderophyllite as dominating end-members. Based on the petrographical observations, it is proposed that the dark mica was formed at a rather late stage in the evolution of the parental rock, i.e. under granulite facies conditions.

Key-words oxyannite, *oxy-ferrokinoshitalite*, calcic gneiss, Scandinavian Caledonides

1. Introduction

Barium-rich micas are known from magmatic rocks (e.g. Bigi et al. 1993; Edgar 1992; Gaspar, Wyllie 1982; Kogarko et al. 2005; Mansker et al. 1979; Thompson 1977;

Wendlandt 1977; Zhang et al. 1993), metamorphosed ore deposits (Chabu, Baulège 1992; Dasgupta et al. 1989; Frimmel et al. 1995; Frondel, Ito 1967; Gnos, Armbruster 2000; Holstam, Larsson 2000; Matsubara et al. 1976; Yoshii et al. 1973a, Tracy 1991) and metamorphic rocks (e.g. Bol et al. 1989; Bucher-Nurminen 1982; Glassley 1975; Harlow 1995; Kretz 1980; Pattiaratchi et al. 1967; Rice 1977; Solie, Su 1987; Tracy, Beard 2003). The latter are mainly represented by low- to moderate-pressure granulite facies rocks or metasomatites.

There are few known brittle micas with Ba substituting for K. Probably the most well-known, and likely the most common, is kinoshitalite, first reported by Yoshii et al. (1973) from the Noda-Tamagawa mine, where metamorphosed sedimentary chert-hosted Mn ores occur. Kinoshitalite was also later found in, e.g. granulite-facies Mn ore from Oman (Gnos, Armbruster 2000). Guggenheim and Frimmel (1999) reported ferrokinoshitalite, the Fe^{2+} analogue, in material from the massive Pb-Zn-Cu-Ag sulfide orebody of the Broken Hill mine, South Africa. Oxykinoshitalite, which may be deemed the Ti-rich and O-analogue of kinoshitalite, was described by Kogarko et al. (2005) from the volcanic Fernando de Oronha island, Brazil. Anandite, the unique sulphide-bearing Ba-Fe mica, was discovered in the Wilagedera prospect, Sri Lanka, where it forms veinlets and lenses within magnetite ore (Pattiaratchi 1967). Ganterite, the Ba analogue of muscovite, was reported by Graeser et al. (2003) from metamorphic rocks in the Berisal Complex in Switzerland and named after the Ganter valley of the Simplon area. The mica highly enriched in Ba that we report on here occurs in ultra-high pressure (UHP) metasediments intercalated with diamond-bearing paragneisses.

2. Geological setting, sample location and description

The Seve Nappe Complex of the Scandinavian Caledonides forms a part of the Middle Allochthon that once formed a continent-ocean transition zone of the Baltican extended margin (e.g. Gee et al. 2013). These rocks experienced deep subduction, locally reaching UHP conditions (e.g. Brueckner et al. 2004; Gilio et al. 2015; Janák et al. 2013; Klonowska et al. 2014, 2016) due to the Iapetus Ocean closure (e.g. Gee et al. 2013). This deep burial of the Baltican margin resulted in the formation of eclogites and garnet peridotites as well as diamond-bearing gneisses (Klonowska et al. 2015; Majka et al. 2014). Such diamond-bearing gneisses occur at Tväråklumparna in the Snasahögarna Mts of Jämtland in Sweden. The sample discussed in this study was collected there (63.20435, 12.35096). The gneisses constitute a monotonous sequence of metapelitic-metapsammitic lithologies intercalated with less common calc-silicate rocks and marbles.

The rock investigated is a garnet-bearing calcic gneiss collected from the same locality as the diamond-bearing gneiss described by Majka et al. (2014). It contains garnet, clinopyroxene, phengitic muscovite, K-feldspar, plagioclase, dark mica, quartz, kyanite and sillimanite as main phases. Calcite, zircon, rutile, titanite, graphite, pyrite and manganoan ilmenite occur in accessory amounts. Porphyroblasts of garnet and clinopyroxene are embedded in a strongly foliated quartz and feldspar matrix with quartz bands separating porphyroblastic segments. Late amphibole and chlorite surround clinopyroxene. Kyanite forms rare lenses overgrown by later sillimanite that is, in turn, surrounded by fibrolite. Muscovite decomposes to quartzofeldspathic symplectites that are interpreted as effects of

partial melting. The dark mica forms relatively fresh, well-developed euhedral to subhedral laths, typically ca. 200 µm long (Fig. 1), which are oriented parallel to subparallel to the main foliation. Modal proportions of the mica are < 0.5%. In rare cases, it is partly replaced or overgrown by K-feldspar and occasionally by amphibole. Dark mica laths are commonly observed along straight feldspar grain boundaries associated with ilmenite and muscovite breakdown textures where muscovite is replaced by plagioclase. Some dark micas are enclosed in plagioclase. Together, the associated phases form triple junctions with sharp grain contacts. Based on the petrography, it is evident that the rock underwent high pressure metamorphism followed by decompression to granulite facies conditions associated with partial melting. This was followed by further decompression and cooling under amphibolite facies conditions. Textural relations together with minor amounts of BaO in muscovite (ca. 0.5wt%) indicate that the Ba-rich dark mica grew cogenetically with ilmenite and feldspar at the expense of phengitic muscovite.

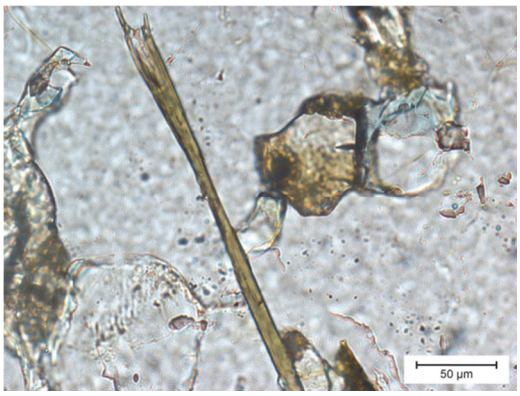

Fig. 1. Photomicrograph of the dark mica from the Tväråklumparna gneiss.

3. Methods

Mineral chemistry was determined using a Jeol JXA8530F Hyperprobe Field Emission Electron Probe Microanalyser (FE-EPMA) at the Centre for Experimental Mineralogy, Petrology and Geochemistry (CEMPEG), Uppsala University, Sweden. Operating conditions during the analyses were as follows: 10 nA beam current with 15 kV accelerating voltage and counting times of 10 s on peaks and 5 s on ±background positions. Mineral standards: Ca – wollastonite, Si – wollastonite, Na – albite, K – orthoclase, Mn and Ti – pyrophanite, Fe – fayalite, Mg – MgO, Ba – barite, S – sphalerite, F – griceite, Al – Al_2O_3 and Cr – Cr_2O_3 were used for calibration. Kα spectral lines were measured for all elements except for Ba which was measured using the Lα line. Beam size was defocused to 10-15 µm to decrease the damage. Raw counts were corrected using the PAP routine.

4. Results

The results of the microprobe analyses of the mica, together with calculated end members, are given in Table 1. The mica is strongly enriched in both Ba and Ti. Contents

of both Ba and Ti are relatively constant: 9.53-13.38wt% BaO with mean of 11.54 and 6.67-8.45wt% TiO_2 with mean of 7.80wt%. The mean crystallochemical formula (n=64) for the analyzed mica is: $(K_{0.54}Ba_{0.39}Na_{0.02}Ca_{0.01})_{\Sigma 0.96}(Fe_{1.37}Mg_{0.85}Ti_{0.50}Al_{0.29}Mn_{0.01}Cr_{0.01})_{\Sigma 3.03}(Si_{2.59}Al_{1.41})_{\Sigma 4.00}O_{10}(OH_{1.30}O_{0.66}F_{0.02}S_{0.01})_{\Sigma 1.99}$. All iron was considered to be dioctahedral. The formula was calculated based on the observations listed below.

(1) Negative Ba-K correlation is high (Fig. 2a) with $r^2 = 0.84$.
(2) Ti correlates negatively with Mg+Fe+^{VI}Al (Fig. 2b) with $r^2 = 0.88$, confirming its location at one of the octahedral sites.
(3) The negative correlation of Ti with Mg (Fig. 2c) and its $r^2 = 0.84$ suggests Ti-Mg substitution at the M1 site according to the $TiMg_{-2}$ exchange vector. Simultaneously, the positive correlation of Ti with Fe with r^2 of 0.78 (Fig. 2c) indicates that Fe occupies only the *M*2 site.
(4) The Ti-Mg substitution is also confirmed by the trends observed in the R^{2+}+Si *vs* Ti^{4+}+$2Al^{3+}$ diagram (Fig. 2d; $r^2 = 0.94$) and in the R^{2+}+$2OH^-$ *vs* Ti^{4+}+$2O^{2-}$ diagram (Fig. 2e; $r^2 = 0.99$). These diagrams correspond to the Ti-Tschermak's and Ti-oxy substitution schemes, respectively (Bol et al. 1989). In the light of these observations, Mg was allocated, between the *M*2 and *M*1 sites;
(5) The negative correlation of Fe and Mg (Fig. 2f) has a high r^2 of 0.93;
(6) If ^{IV}Al and Si are plotted against Ti (Fig. 3), the relatively scattered r^2 values (< 0.5) of the regression lines point to the absence of Ti at the tetrahedral sites.

The mean TiO_2 content of 7.80 wt% is high enough to include *oxyannite*[1] (Oan) $KFe_2Ti(AlSi_3O_{10})O_2$, oxyphlogopite (Oph) $KMg_2Ti(AlSi_3O_{10})O_2$ and oxykinoshitalite (Oks) $BaMg_2Ti(Al_2Si_2O_{10})O_2$ in the mica composition. The main end member is *oxyannite* (see also Fig. 4a). The data obtained fall close to the join of the Fe-biotite and siderophyllite fields in the Mg-(Al+Ti)-(Fe+Mn) diagram of Foster (1960; Fig. 4b). Hypothetical $BaFe_2Mg(Al_2Si_2O_{10})(OH)_2$ (Bfm), $BaFe_2Al(AlSi_3O_{10})O_2$ (Bfa), $BaMg_2Al(AlSi_3O_{10})O_2$ (Bma) and *oxy-ferrokinoshitalite* (Ofk) $BaFe_2Ti(Al_2Si_2O_{10})O_2$ components are also involved. Minor components (usually with 1% abundance) include hypothetical *oxyferroaspidolite* $NaFe_2Ti(AlSi_3O_{10})O_2$ and *ferroaspidolite* $NaFe_2Mg(AlSi_3O_{10})(OH)_2$, accompanied by fluorannite and fluorphlogopite. The low content of S precludes anandite from entering the composition. The presence of the yangzhumingite $KMg_{2.5}(Si_4O_{10})F_2$ component is considered unlikely due to both the strong ^{IV}Al-Si substitution and the undersaturation in F. All Al is allocated to the *M*1 site because of the high amounts of Fe and ^{M2}Mg. The main empirical formula above was recast using the following additional K-rich end-members: "annite-phlogopite" (Aph), phlogopite (Phl), siderophyllite (Sdp) $KFe_2Al(AlSi_3O_{10})(OH)_2$ and its Mg-analogue – eastonite (Eas). The mean end-member formula should be expressed as $Oan_{19}Ofk_{14}Sdp_{11}Oph_9Aph_8Bfa_8Bfm_6Oks_6Phl_4Bma_4Eas_3Ksh_3R_5$, with R standing for the remaining end-members[2].

[1] names of the hypothetical components, not approved by the International Mineralogical Association (IMA), are *italicized*
[2] Analytical and calculation uncertainties may also be responsible for lower summation

Table 1. Representative WDS analyses of Ba-Ti-rich dark mica from Tväråklumparna.

	1	2	3	4	5	6	7	8	9	10	11	12	13	14	15	16	17	18
wt.%																		
SiO_2	29.25	29.33	30.99	30.60	29.77	30.61	31.22	31.43	32.25	32.54	32.26	31.75	31.51	31.93	32.06	31.80	31.42	30.13
TiO_2	8.05	8.05	8.04	8.34	8.20	8.13	7.69	7.15	6.89	6.72	7.04	7.07	6.90	6.80	6.81	6.67	7.10	7.92
Cr_2O_3	0.06	0.06	0.07	0.07	0.07	0.06	0.05	0.05	0.06	0.06	0.06	0.05	0.07	0.06	0.06	0.06	0.05	0.09
Al_2O_3	17.25	17.31	16.69	16.54	16.31	16.68	16.92	16.71	16.71	16.60	16.45	16.56	16.55	16.72	16.52	16.70	16.98	16.68
FeO	20.89	20.26	18.21	18.47	18.68	18.24	17.65	17.79	17.41	17.69	17.76	17.94	17.66	17.60	17.67	17.36	17.58	19.40
MnO	0.13	0.07	0.01	0.05	0.00	0.00	0.03	0.03	0.04	0.00	0.09	0.07	0.09	0.04	0.08	0.08	0.06	0.24
MgO	5.42	5.33	7.13	6.69	6.84	6.77	7.28	7.91	8.29	8.68	8.26	8.13	8.30	8.34	8.52	8.61	7.91	6.51
BaO	12.34	12.42	12.47	13.38	13.05	12.91	11.75	10.53	9.96	9.60	10.06	10.23	9.99	9.86	9.78	9.53	10.05	10.19
CaO	0.12	0.15	0.03	0.05	0.05	0.04	0.01	0.01	0.05	0.09	0.23	0.08	0.08	0.01	0.01	0.03	0.04	0.15
Na_2O	0.24	0.05	0.00	0.10	0.05	0.16	0.07	0.08	0.06	0.05	0.09	0.11	0.04	0.07	0.08	0.06	0.06	0.23
K_2O	4.64	4.57	4.57	4.27	4.34	4.43	4.90	5.32	5.44	5.56	5.40	5.39	5.38	5.57	5.75	5.74	5.40	5.42
F	0.06	0.14	0.03	0.00	0.04	0.09	0.02	0.29	0.12	0.30	0.13	0.13	0.19	0.27	0.05	0.16	0.10	0.00
Cl	0.00	0.01	0.02	0.03	0.03	0.03	0.02	0.01	0.02	0.02	0.00	0.02	0.03	0.02	0.01	0.01	0.02	0.01
S[1)]	0.11	0.11	0.04	0.06	0.08	0.08	0.07	0.05	0.08	0.05	0.06	0.07	0.10	0.07	0.09	0.07	0.07	0.06
Σ	98.56	97.86	98.30	98.64	97.51	98.24	97.67	97.37	97.39	97.95	97.90	97.60	96.89	97.36	97.49	96.87	96.83	97.03
H_2O[2)]	1.44	2.14	1.70	1.36	2.49	1.76	2.33	2.63	2.61	2.05	2.10	2.40	3.11	2.65	2.51	3.13	3.17	2.97
apfu (base: 8 cations)																		
Si	2.52	2.55	2.65	2.63	2.59	2.63	2.66	2.66	2.71	2.71	2.70	2.67	2.66	2.68	2.68	2.67	2.66	2.58
Ti	0.52	0.53	0.52	0.54	0.54	0.53	0.49	0.46	0.44	0.42	0.44	0.45	0.44	0.43	0.43	0.42	0.45	0.51
Cr	0.00	0.00	0.00	0.00	0.00	0.00	0.00	0.00	0.00	0.00	0.00	0.00	0.00	0.00	0.00	0.00	0.00	0.01
^{IV}Al	1.48	1.45	1.35	1.37	1.41	1.37	1.34	1.34	1.29	1.29	1.30	1.33	1.34	1.32	1.32	1.33	1.34	1.42
^{VI}Al[3)]	0.27	0.33	0.34	0.31	0.26	0.32	0.37	0.33	0.36	0.34	0.32	0.31	0.31	0.34	0.31	0.32	0.35	0.26
Fe[4)]	1.50	1.47	1.30	1.33	1.36	1.31	1.26	1.26	1.22	1.23	1.24	1.26	1.25	1.24	1.23	1.22	1.24	1.39
Mn	0.01	0.00	0.00	0.00	0.00	0.00	0.00	0.00	0.00	0.00	0.01	0.01	0.01	0.00	0.01	0.01	0.00	0.02
^{M2}Mg	0.50	0.53	0.70	0.67	0.64	0.69	0.74	0.74	0.78	0.77	0.76	0.74	0.75	0.76	0.77	0.78	0.76	0.61
^{M1}Mg	0.20	0.17	0.21	0.19	0.25	0.18	0.19	0.26	0.26	0.31	0.27	0.28	0.30	0.28	0.30	0.30	0.24	0.22
Ba	0.42	0.42	0.42	0.45	0.44	0.44	0.39	0.35	0.33	0.31	0.33	0.34	0.33	0.32	0.32	0.31	0.33	0.34
Ca	0.01	0.01	0.00	0.00	0.00	0.00	0.00	0.00	0.00	0.01	0.02	0.01	0.01	0.00	0.00	0.00	0.00	0.01

Table 1. - continuation																		
Na	0.04	0.01	0.00	0.02	0.01	0.03	0.01	0.01	0.01	0.01	0.01	0.02	0.01	0.01	0.01	0.01	0.01	0.04
K	0.51	0.51	0.50	0.47	0.48	0.49	0.53	0.58	0.58	0.59	0.58	0.58	0.58	0.60	0.61	0.61	0.58	0.59
F	0.02	0.04	0.01	0.00	0.01	0.03	0.01	0.08	0.03	0.08	0.03	0.03	0.05	0.07	0.01	0.04	0.03	0.00
OH	0.83	1.22	0.95	0.77	1.43	0.99	1.30	1.47	1.45	1.12	1.16	1.33	1.75	1.47	1.38	1.74	1.78	1.68
O	1.14	0.72	1.03	1.22	0.54	0.97	0.68	0.44	0.51	0.79	0.80	0.62	0.19	0.45	0.59	0.20	0.18	0.31
S	0.02	0.02	0.01	0.01	0.01	0.01	0.01	0.01	0.01	0.01	0.01	0.01	0.02	0.01	0.01	0.01	0.01	0.01
end members [%]																		
Oan[4)]	20	20	17	17	18	17	17	17	16	16	16	17	16	16	16	16	17	21
Ofk	17	17	14	16	16	15	12	10	9	8	9	10	9	9	9	8	10	12
Sdp	11	12	11	10	9	10	12	12	13	12	12	12	12	13	12	12	13	11
Oph	7	7	9	9	8	9	10	10	10	10	10	10	10	10	10	10	10	9
Aph	8	6	7	6	8	6	6	10	9	11	10	10	11	11	11	11	9	9
Bfa	9	10	9	10	8	9	9	7	7	7	7	7	7	7	6	6	7	6
Bfm	6	5	6	6	8	5	5	6	5	6	6	6	6	6	6	6	5	5
Oks	5	6	8	8	8	8	7	6	6	5	6	6	6	5	5	5	6	5
Phl	3	2	4	3	4	3	4	6	6	7	6	6	7	6	7	7	5	4
Bma	2	2	3	3	3	2	3	3	3	3	3	3	3	3	3	3	3	2
Eas	3	4	6	5	4	6	7	7	8	8	7	7	7	8	7	8	8	5
Ksh	2	2	3	3	4	3	3	3	3	4	3	4	4	4	4	4	3	2

[1)] S was measured as SO_3 and then recalculated to S; [2)] calculated as 100- Σ; ^{VI}Al is located at the *M*1 site; [3)] all Fe is assumed to be dioctahedral; [4)] please see the main text for explanations

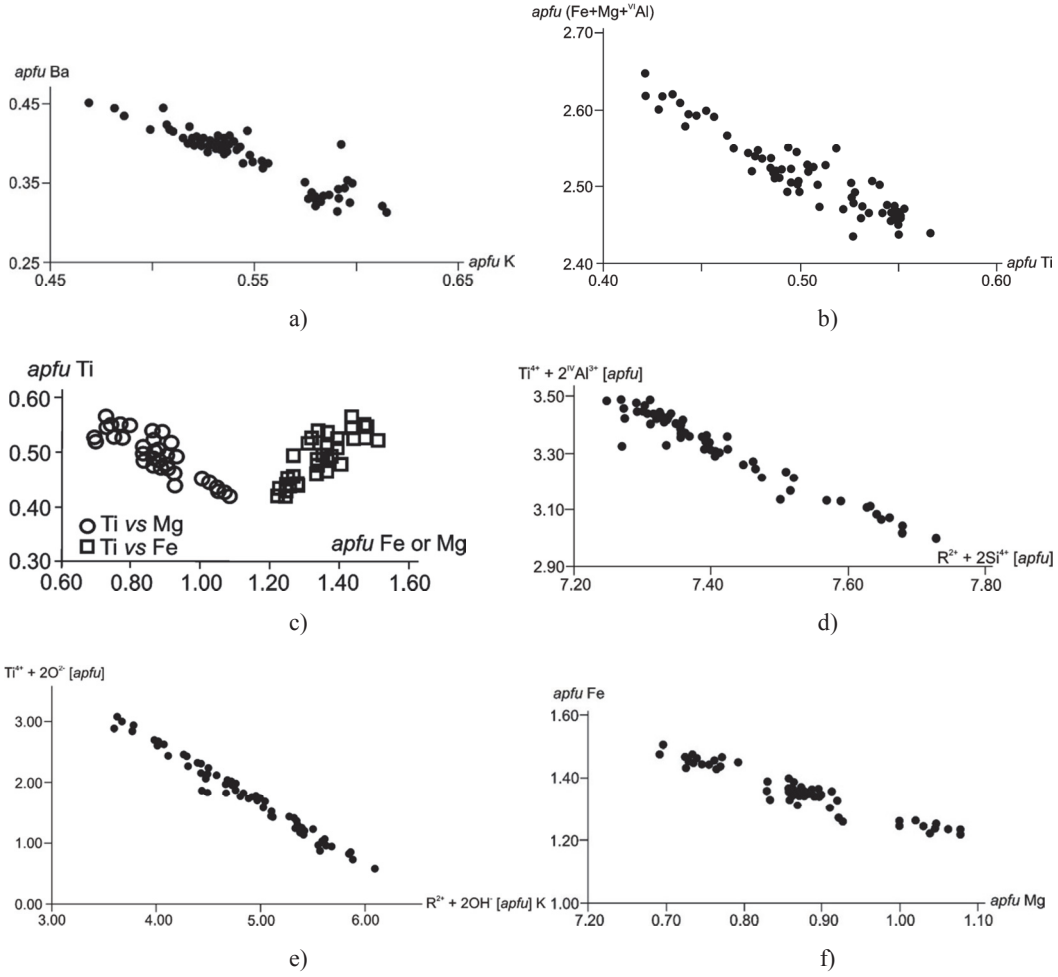

Fig. 2. Diagrams of (a) Ba *vs* K, (b) (Mg+Fe+^{VI}Al) *vs* Ti, (c) Ti *vs* Mg and Ti vs. Fe, (d) Ti^{4+}+$2Al^{3+}$ *vs* R^{2+}+Si, (e) Ti^{4+}+$2O^{2-}$ *vs* R^{2+}+$2OH^{-}$ and (f) Fe *vs* Mg correlations in the dark mica.

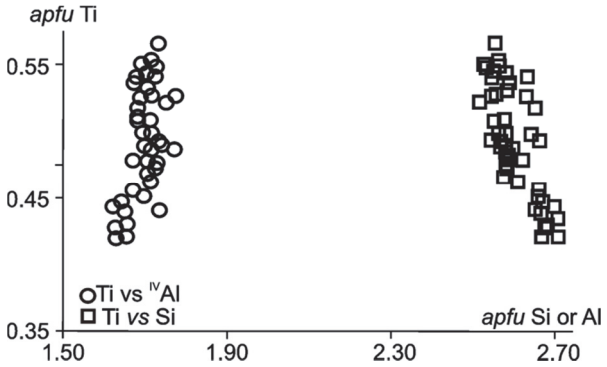

Fig. 3. Diagram of Ti *vs* ^{IV}Al and Ti *vs* Si showing weak correlation between these cations.

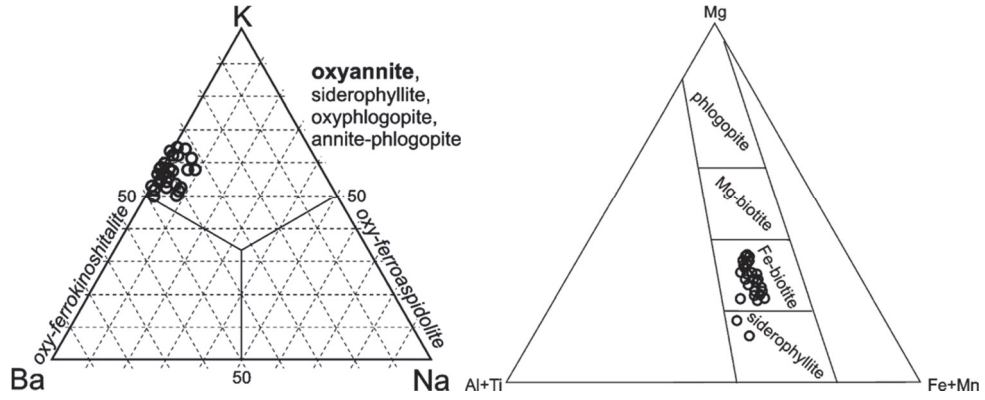

a) b)

Fig. 4. Dark mica classification diagrams: (a) Ba-K-Na and (b) (Al+Ti)-Mg-(Fe+Mn), from Foster (1960).

5. Final remarks

The mica described is clearly enriched in Ba and Ti. The fact that both constituents correlate positively may point to a common source for both. Taking account of the character of the protolith of the parental rock, it can be speculated that this rock could have acted as a source for these elements. Such Ba- and Ti-enriched micas occurring in metamorphic rocks have been described from a very few places worldwide. For example, kinoshitalite is known from relatively high temperature (> 600^{o}C), but not high pressure, metasediments in the Alaska Range (Solie, Su 1987). Marbles and skarns in Virginia are also a source of Mn-rich kinoshitalite (Tracy, Beard 2003). Frimmel et al. (1995) reported the Fe-analogue of kinoshitalite among other Ba-bearing micas from upper amphibolite to granulite facies rocks in the Namaqualand Complex, South Africa, where mica-bearing banded-iron-formation rocks coexists with sulphide ore bodies. Kinoshitalite has also been described from granulite facies manganese ores in Oman (Gnos, Armbruster 2000). Bol et al. (1989) reported Ba- and Ti-rich phlogopite from Rogaland marbles that formed under extremely dry granulite-facies conditions. Importantly, the mica studied here is somewhat similar to that described by Bol et al. (1989); it also occurs in carbonate-bearing rocks.

The calcic gneiss in the Tväråklumparna locality is, to our knowledge, the first known UHP metasediment carrying such a Ba-enriched dark mica. However, it is not certain whether the studied mica was stable at the peak pressure conditions or not. The rocks of the Seve Nappe Complex underwent an extensive high- to moderate-pressure granulite-facies overprinting during exhumation from the UHP setting (e.g. Klonowska et al. 2014). This process was associated with phengitic-mica decompression melting. This white mica was the most probable source of Ba for the newly-formed dark mica. The fact that the mica is well preserved and typically occurs as undeformed euhedral to subhedral laths may indeed reflect relatively late growth, probably under granulite facies conditions postdating the peak pressure metamorphic stage.

Acknowledgements. Igor Petrík, Adam Szuszkiewicz and an anonymous reviewer are thanked for their constructive comments on this paper. Marek Michalik is acknowledged for the editorial handling. This study was supported by Swedish Research Council (VR) project no. 2012-4441 to JM.

6. References

Bigi, S., Brigatti, M.F., Mazzucchelli, M., & Rivalenti, G. (1993). Crystal chemical variations in Ba-rich biotites from gabbroic rocks of lower crust Ivrea zone, NW Italy. *Contributions to Mineralogy and Petrology,* 113, 87–99. DOI: 10.1007/BF00320833.

Bol, L.C.G.M., Bos, A., Sauter, P.C.C., & Jansen, J.B.H. (1989). Barium-titanium-rich phlogopites in marbles from Rogaland, southwest Norway. *American Mineralogist,* 74, 439–447. DOI: 0003-004v89/03044439$02.00.

Brueckner, H.K., Van Roermund, H.L.M., & Pearson, N. (2004). An Archean to Paleozoic evolution for a garnet peridotite lens with sub-Baltic Shield affinity within the Seve Nappe Complex of Jämtland, Sweden, Central Scandinavian Caledonides. *Journal of Petrology*, 45, 415–437. DOI: 10.1093/petrology/egg088.

Bucher-Nurminen, K. (1982). Mechanism of mineral reactions inferred from textures of impure dolomitic marbles from East Greenland. *Journal of Petrology*, 23, 325–343. DOI: 10.1093/petrology/23.3.325.

Chabu, M. & Baulège, J. (1992). Barian feldspar and muscovite from Kingushi Zn-Pb-Cu deposit, Shaba, Zaire. *Canadian Mineralogist*, 30, 1143–1152.

Dasgupta, S., Chakraborti, S., Sengupta, P., Bhattacharya, P.K., Banerjee, H., & Fukuoka, M. (1989). Compositional characteristics of kinoshitalite from the Sausar Group, India. *American Mineralogist*, 74, 200–202.

Edgar, A.D. (1992). Barium-rich phlogopite and biotite from some Quaternary alkali mafic lavas, West Eifel, Germany. *European Journal of Mineralogy*, 4, 321–330.

Foster M.D. (1960). *Interpretation of the composition of trioctahedral micas.* Geological Survey Professional Paper 354-B, 49 pp.

Frimmel, H.E., Hoffmann, D., Watkins, R.T., & Moore, J.M. (1995). An Fe analogue of kinoshitalite from the Broken Hill Massie sulfide deposit in the Namaqualand Metamorphic Complex, South Africa. *American Mineralogist*, 80, 833–840. DOI: 10.2138/am-1995-7-819.

Frondel, C. & Ito, J. (1967). Barium-rich phlogopite from Långban, Sweden. *Arkiv för Mineralogi och Geologi*, 4, 445–447.

Gaspar, J.C. & Wyllie, P.J., 1982. Barium phlogopite from the Jacupiranga carbonatite, Brazil. *American Mineralogist*, 67, 997–1000.

Gee, D.G., Janák, M., Majka, J., Robinson, P., & Van Roermund, H. (2013). Subduction along and within the Baltoscandian margin during closing of the Iapetus Ocean and Baltica-Laurentia collision. *Lithosphere*, 5, 169–178. DOI: 10.1130/L220.1.

Gilio, M., Clos, F., & van Roermund, H.L.M. (2015). The Friningen Garnet Peridotite (central Swedish Caledonides). A good example of the characteristic PTt path of a cold mantle wedge garnet peridotite. *Lithos*, 230, 1–16. DOI: 10.1016/j.lithos.2015.05.003.

Glassley, W.E. (1975). High grade regional metamorphism of some carbonate bodies: significance for the orthopyroxene isograd. *American Journal of Science*, 275, 1133–1163.

Gnos, E. & Armbruster, T. (2000). Kinoshitalite, $Ba(Mg)_3(Al_2Si_2)O_{10}(OH,F)_2$, a brittle mica from a manganese deposit in Oman: Paragenesis and crystals chemistry. *American Mineralogist*, 85, 242–250. DOI: 0003-004X/00/0001–0242$05.00.

Graeser, S., Hetherington, C.J., & Gieré, R. (2003). Ganterite, a new barium-dominant analogue of muscovite from the Berisal Complex, Simplon Region, Switzerland. *Canadian Mineralogist*, 41, 1271–1280. DOI: 10.2113/gscanmin.41.5.1271.

Guggenheim, S., & Frimmel, H.E. (1999). Ferrokinoshitalite, a new species of brittle mica from the Broken Hill mine, South Africa: structural and mineralogical characterization. *Canadian Mineralogist*, 37, 1445–1452.

Harlow, G.E. (1995). Crystal chemistry of barian enrichment in micas from metasomatized inclusions in serpentinite, Motagua Fault Zone, Guatemala. *European Journal of Mineralogy*, 7, 775–790. DOI: 10.1127/ejm/7/4/0775.

Holstam, D., & Larsson A.K. (2000). Tegengrenite, a new, rhombohedral spinel-related Sb mineral from the Jakobsberg Fe-Mn deposit, Värmland, Sweden. *American Mineralogist*, 85, 1315–1320. DOI: http://dx.doi.org/10.2138/am-2000-8-926.

Janák, M., Van Roermund, H.L.M., Majka, J. & Gee, D.G. (2013). UHP metamorphism recorded by kyanite-bearing eclogite in the Seve Nappe Complex of northern Jämtland, Swedish Caledonides. *Gondwana Research*, 23, 865-879. DOI: 10.1016/j.gr.2012.06.012.

Klonowska, I., Janák, M., Majka, J., Froitzheim, N., & Gee, D.G. (2015). The UHP metamorphic Seve Nappe Complex of the Swedish Caledonides - a new occurrence of the microdiamond-bearing gneisses and their exhumation. *Geophysical Research Abstracts*, 17, EGU2015-11609.

Klonowska, I., Majka, J., Janák, M., Gee, D.G., & Ladenberger, A. (2014*).* Pressure-temperature evolution of a kyanite-garnet pelitic gneiss from Åreskutan: evidence of (U)HP metamorphism of the Seve Nappe Complex, west-central Jämtland, Swedish Caledonides. 390, 321–336. DOI: 10.1144/SP390.7 In: Corfu, F., Gasser, D. & Chew, D. M. (eds) New Perspectives on the Caledonides of Scandinavia and Related Areas*. Geological Society, London, Special Publications*.

Kogarko, L.A., Uvarova, Y.A., Sokolova, E., Hawthorne, F.C., Ottolini, L., & Grice, J.D. (2005). Oxykinoshitalite, a new species of mica from Fernando de Noronha island, Pernambuco, Brazil: occurrence and crystal structure. *Canadian Mineralogist*, 43, 1501–1510. DOI: 10.2113/gscanmin.43.5.1501.

Kretz, R. (1980). Occurrence, mineral chemistry and metamorphism of Precambrian carbonate rock in a portion of the Grenville Province. *Journal of Petrology*, 21, 573–620.

Majka, J., Rosén, Å., Janák, M., Froitzheim, N., Klonowska, I.,Manecki, M., Sasinková, V., & Yoshida, K. (2014). Microdiamond discovered in the Seve Nappe (Scandinavian Caledonides) and its exhumation by the "vacuum-cleaner" mechanism. *Geology*, 42, 1107–1110. DOI: 10.1130/G36108.1.

Mansker, W.L., Ewing, R.C., & Keil, K. 1979. Barian-titanian biotites in nephelinites from Oahu, Hawaii. *American Mineralogist*, 64, 156–159.

Manuella, F.C., Carbone, S., Ottolini, L., & Gibilisco, S. (2012). Micro-Raman spectroscopy and SIMS characterization of oxykinoshitalite in an olivine nephelinite from the Hyblean Plateau (Sicily, Italy). *European Journal of Mineralogy*, 24, 527–533. DOI: 10.1127/0935-1221/2012/0024-2191.

Matsubara, S., Kato, A., Nagashima, A., & Matsuo, G. (1976). The occurrence of kinoshitalite from Hokkejino, Kyoto Prefecture, Japan. *Bulletin of the Natural Science Museum Series C*, 2, 71–78.

Pattiaratchi, D.B., Saari, E., & Sahama, T.G. (1967). Anandite, a new barium iron silicate from Wilagedera, North Western Province, Ceylon. *Mineralogical Magazine*, 36, 1–4.

Rice, J.M. (1977). Progressive metamorphism of impure dolomitic limestone in the Marysville aureole, Montana. *American Journal of Science*, 277, 1–24.

Solie, D.N. & Su, S.C. 1987. An occurrence of Ba-rich micas from the Alaska Range. *American Mineralogist*, 72, 995–999.

Thompson, R.N. (1977). Primary basalts and magma genesis. III Alban Hills, Roman comagmatic province, Central Italy. *Contributions to Mineralogy and Petrology*, 60, 91–108.

Tracy, R.J. (1991). Ba-rich micas from the Franklin marble, Lime Crest and Sterling Hill, New Jersey. *American Mineralogist*, 76, 1683–1693.

Tracy, R.J. & Beard, J.S., 2003. Manganoan kinoshitalite in Mn-rich marble and skarn from Virginia. *American Mineralogist*, 88, 740–747.

Wendlandt, R.F. (1977). Barium-phlogopite from the Jaystack Butte, Highwood Mountains, Montana. *Carnegie Institution Washington, Year Book*, 76, 534–539.

Yoshii, M., Maeda, K., Kato, T., Watanabe, T., Yui, S., Kato, A. & Nagashima, K. (1973). Kinoshita1ite, a new mineral from the Noda-Tamagawa mine, Iwate Prefecture. *Chigaku Kenkyu*, 24, 181−190 (in Japanese).

Zhang, M., Suddaby, P., Thompson, R.N. & Dungan, M.A. (1993). Barian-titanian phlogopite from potassic lavas in northwest China: chemistry, substitutions and paragenesis. *American Mineralogist*, 78, 1056–1065.